



# Methylpiperidinium Iodides as Novel Antagonists for $\alpha 7$ Nicotinic Acetylcholine Receptors

Jhon J. López<sup>1\*</sup>, Jesús García-Colunga<sup>2\*</sup>, Edwin G. Pérez<sup>3</sup> and Angélica Fierro<sup>3</sup>

<sup>1</sup> Department of Chemistry, Faculty of Sciences, University of Chile, Santiago, Chile, <sup>2</sup> Departamento de Neurobiología Celular y Molecular, Instituto de Neurobiología, Universidad Nacional Autónoma de México, Mexico City, Mexico, <sup>3</sup> Department of Organic Chemistry, Faculty of Chemistry, Pontificia Universidad Católica de Chile, Santiago, Chile

## OPEN ACCESS

### Edited by:

Antonio Ferrer-Montiel,  
Universidad Miguel Hernández  
de Elche, Spain

### Reviewed by:

Antonio R. Artalejo,  
Complutense University of Madrid,  
Spain

Rosario Gonzalez-Muniz,  
Instituto de Química Médica (IQM),  
Spain

### \*Correspondence:

Jhon J. López  
jjlopez@uc.cl  
Jesús García-Colunga  
garciaacolunga@unam.mx

### Specialty section:

This article was submitted to  
Pharmacology of Ion Channels  
and Channelopathies,  
a section of the journal  
Frontiers in Pharmacology

**Received:** 18 April 2018

**Accepted:** 19 June 2018

**Published:** 10 July 2018

### Citation:

López JJ, García-Colunga J,  
Pérez EG and Fierro A (2018)  
Methylpiperidinium Iodides as Novel  
Antagonists for  $\alpha 7$  Nicotinic  
Acetylcholine Receptors.  
Front. Pharmacol. 9:744.  
doi: 10.3389/fphar.2018.00744

The  $\alpha 7$  nicotinic acetylcholine receptor (nAChR) is expressed in neuronal and non-neuronal cells and is involved in several physiopathological processes, and is thus an important drug target. We have designed and synthesized novel piperidine derivatives as  $\alpha 7$  nAChR antagonists. Thus, we describe here a new series of 1-[2-(4-alkoxy-phenoxy-ethyl)]piperidines and 1-[2-(4-alkoxy-phenoxy-ethyl)]-1-methylpiperidinium iodides (compounds **11a-11c** and **12a-12c**), and their actions on  $\alpha 7$  nAChRs. The pharmacological activity of these compounds was studied in rat CA1 hippocampal interneurons by using the whole-cell voltage-clamp technique. Inhibition of the choline-induced current was less for **11a-11c** than for the methylpiperidinium iodides **12a-12c** and depended on the length of the aliphatic chain. Those compounds showing strong effects were studied further using molecular docking and molecular dynamics simulations. The strongest and non-voltage dependent antagonism was shown by **12a**, which could establish cation- $\pi$  interactions with the principal (+)-side and van der Waals interactions with the complementary (-)-side in the  $\alpha 7$  nAChRs. Furthermore, compound **11a** forms hydrogen bonds with residue Q115 of the complementary (-)-side through water molecules without forming cation- $\pi$  interactions. Our findings have led to the establishment of a new family of antagonists that interact with the agonist binding cavity of the  $\alpha 7$  nAChR, which represent a promising new class of compounds for the treatment of pathologies where these receptors need to be negatively modulated, including neuropsychiatric disorders as well as different types of cancer.

**Keywords:** nicotinic acetylcholine receptors, nicotinic antagonists, methylpiperidinium iodides, molecular ligand-receptor interactions, the whole-cell voltage-clamp technique, molecular docking, molecular dynamics

## INTRODUCTION

Nicotinic acetylcholine receptors (nAChRs) are membrane proteins belonging to the superfamily of Cys-loop ligand-gated ion channels that include serotonin (5-HT<sub>3</sub>), GABA<sub>A</sub>, GABA<sub>C</sub>, and glycine receptors (Lester et al., 2004; Dineley et al., 2015). They are pentameric structures composed of four different subunits in muscle receptors ( $\alpha 1$ ,  $\beta 1$ ,  $\gamma$  or  $\epsilon$ , and  $\delta$ ), whereas the neuronal subtypes

are assembled as homomeric or heteromeric receptors from diverse combinations of subunits ( $\alpha 2$ - $\alpha 10$  and  $\beta 2$ - $\beta 4$ ) conferring different physiological, pharmacological and biophysical properties (Gotti et al., 2009; Blum et al., 2010; Zoli et al., 2017).

The agonist binding site, known as the “aromatic box,” is located at the interface between two  $\alpha$  subunits [residues Y89, W143, Y185, Y192 of the principal (+)-side and W53 of the complementary (–)-side]; or between one  $\alpha$  subunit [principal (+)-side] and one  $\beta$  subunit [complementary (–)-side, W53] (Olsen et al., 2014). Heteromeric nAChRs with two  $\alpha$  subunits exhibit two binding sites for the agonist, whereas homomeric receptors have five identical binding sites for the agonist (Albuquerque et al., 2009; Gotti et al., 2009).

Of all nAChRs, the  $\alpha 7$ -subtype is one of the most abundant in the nervous system and is involved in several physiological roles, neuropsychiatry and neurodegenerative diseases (Romanelli et al., 2007; Gotti et al., 2009; Dineley et al., 2015). For instance, increased ACh signaling in hippocampus increases depression-like behavior. In addition, the  $\alpha 7$  subunit of nAChR is highly expressed in this region. Thus, under increased ACh conditions, hippocampal  $\alpha 7$  nAChRs may contribute to modulation of depression which can be reversed by the  $\alpha 7$  nAChR antagonists (Mineur et al., 2017).  $\alpha 7$  nAChRs are also present on non-neuronal cells such as bronchial epithelium and keratinocytes (Egleton et al., 2008; Albuquerque et al., 2009; Gahring et al., 2017). On the other hand, tobacco smoking seems to be the chief risk factor for lung, pancreatic, colon, gastric, and bladder cancers (Cooke and Bitterman, 2004; Wong et al., 2007; Egleton et al., 2008), suggesting that nicotine contribute to their pathophysiology. In this regard, several studies have shown that  $\alpha 7$  nAChRs are involved in nicotine-induced proliferation of normal human bronchial epithelial cells, as well as cell proliferation in small cell lung cancer and non-small cell lung cancer, in which  $\alpha 7$  nAChR antagonists decreased these nicotine effects (Heeschen et al., 2002; Trombino et al., 2004; Dasgupta et al., 2006). For these reasons, the  $\alpha 7$  nAChR has been considered as potential pharmacological target, and in the last decades a variety of selective ligands have been synthesized; however, only few compounds are clinically used (Dunbar et al., 2011; Mazurov et al., 2011; Terry et al., 2015). In this sense, the development of selective antagonists for  $\alpha 7$  might be alternative for the treatment of several cancers (Dwoskin and Crooks, 2001; Egleton et al., 2008; Innocent et al., 2008; Peng et al., 2010).

Recently, our group developed the selective antagonists for  $\alpha 7$  nAChRs compounds **1** and **2** (Arias et al., 2013; Pérez et al., 2013; López et al., 2015; **Figure 1**).

There are two important criteria for generating  $\alpha 7$  nAChR antagonists: (a) a center containing a nitrogen atom with a positive charge (cationic center), which can interact with the “aromatic box” of the nAChR. In this regard, the pyridinic nitrogen atom of nicotine (**Figure 2**, compound **3**), alkylated with long aliphatic chains (3–9 atoms of carbon), results in a potent and selective antagonist for nAChRs (**Figure 2**, compounds **4** and **5**) (Crooks et al., 1995; Wilkins et al., 2002); (b) and alkyl groups located at the “para” position of an aromatic ring, which are important for van der Waals interactions with the amino acid residues of the complementary (–)-side, relevant for the

selectivity toward the  $\alpha 7$  subtype (Crooks et al., 1995; Arias et al., 2013; Pérez et al., 2013).

Additionally, a simple piperidine ring has been used for generating selective agonists for  $\alpha 7$  nAChRs (**Figure 2**, compounds **6** and **7**) (Ghiron et al., 2010). It is important to mention that the design, synthesis and chemically characterized of new piperidine derivatives (**Figure 3**, **11a–11c** and **12a–12c**) was based on the binding cavity and our main goal was to evaluate a new chemical architecture as potential ligands for the  $\alpha 7$  nAChR. Additionally, their pharmacological activity was tested in native hippocampal  $\alpha 7$  nAChRs, and their interaction with the receptor was studied using molecular docking and molecular dynamics simulations. In summary, these compounds have a piperidine ring (*N*-methylated or not) and include an aromatic ring substituted at the “para” position with alkyl groups containing 6–8 carbon atoms, expected to enhance the selectivity for  $\alpha 7$  nAChRs (Arias et al., 2013; López et al., 2015).

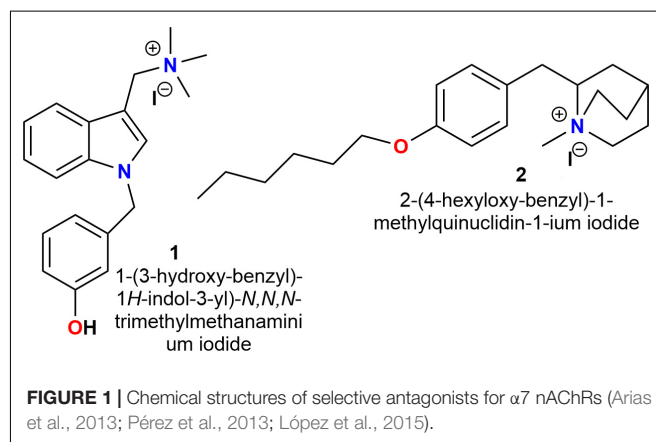
## MATERIALS AND METHODS

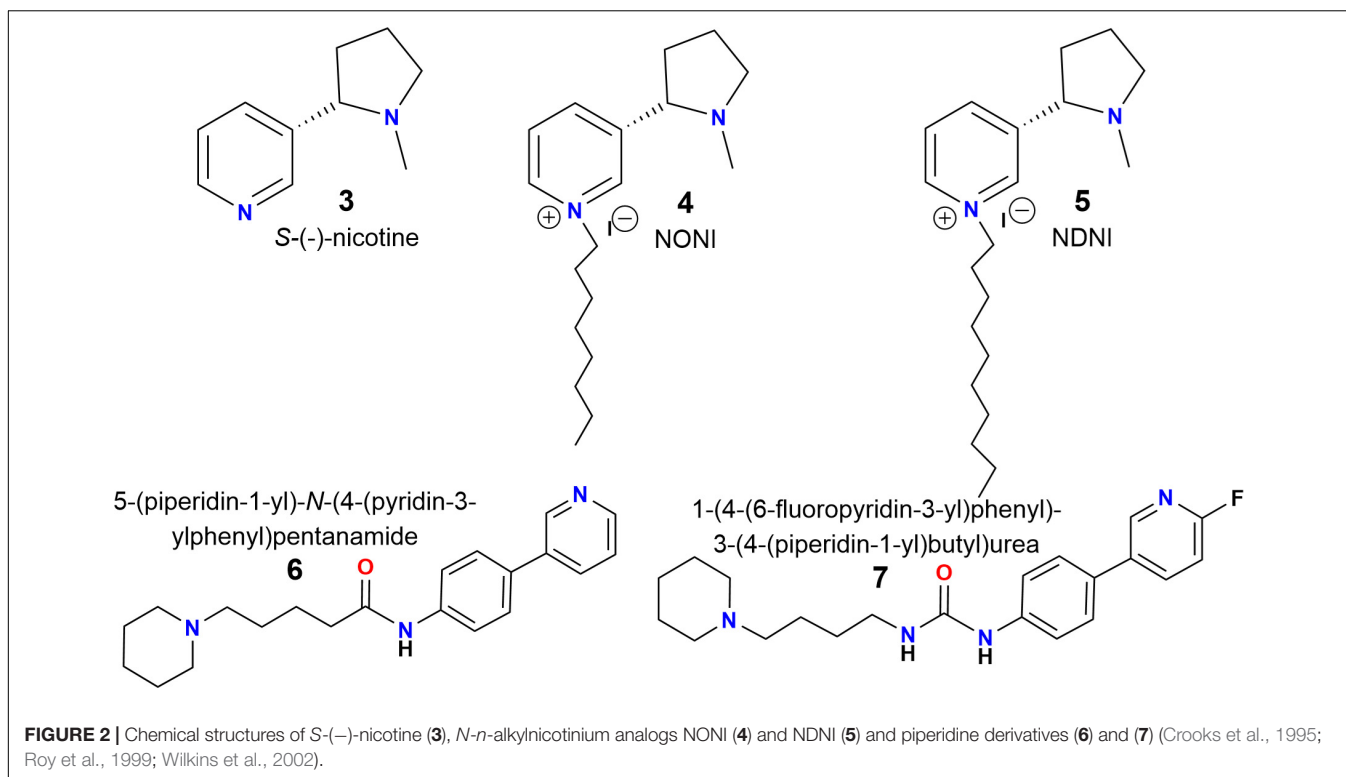
### Chemical Synthesis

For the chemical synthesis of new piperidine derivatives, commercial reagents, and solvents were used (Sigma-Aldrich and MERCK), employing previously described synthetic methodologies (Roy et al., 1999; Peters et al., 2006; Pérez et al., 2012, 2013; Arias et al., 2013; Dang et al., 2016).

### Chemical Characterization

$^1\text{H}$  and  $^{13}\text{C}$  nuclear magnetic resonance (NMR) spectra were recorded at 200 or 400 MHz and 50 or 100 MHz for  $^1\text{H}$  and  $^{13}\text{C}$  respectively, on Bruker ACP-200 or Bruker Avance 400 spectrometers. The results are detailed in the Supplemental Information. Chemical shifts are reported in  $\delta$  values [parts per million (ppm)] relative to an internal standard of tetramethylsilane in deuterated chloroform ( $\text{CDCl}_3$ ) or deuterated methanol ( $\text{CD}_3\text{OD}$ ), and coupling constants (*J*) are given in Hertz. Precoated silica gel 60 plates (Merck 60 F<sub>254</sub> 0.2 mm) were used for thin-layer chromatography and silica gel 60 (0.015–0.040 mm) for column chromatography. Spots





on thin-layer chromatograms were visualized by spraying with Dragendorff's reagent or under ultraviolet light at 254 nm.

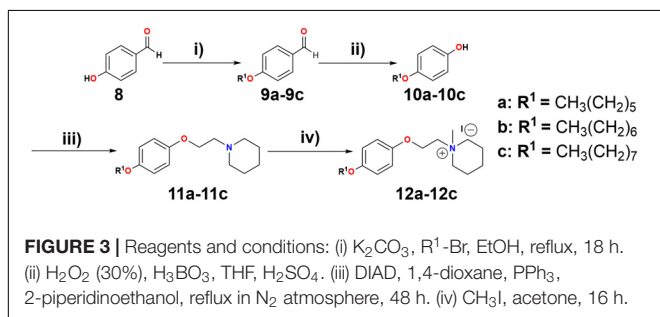
## Electrophysiological Recordings

All experimental procedures were carried out in accordance with the National Institute of Health Guide for Care and Use of Laboratory Animals and were approved by the Institutional Animal Care Committee of the Universidad Nacional Autónoma de México, with an effort to minimize the number of animals used and their suffering. The experiments were performed as previously described (Vázquez-Gómez et al., 2014; López et al., 2015). Briefly, brain slices were obtained from Sprague Dawley rats, 13–16 days after birth. Rats were deeply anesthetized with isoflurane and decapitated. Their brains were removed and placed into an ice cold (4°C) solution containing (in mM): 250 sucrose, 2.5 KCl, 1.2 NaH<sub>2</sub>PO<sub>4</sub>, 5 MgCl<sub>2</sub>, 0.5 CaCl<sub>2</sub>, 26 NaHCO<sub>3</sub>, 10 glucose, pH 7.4. Coronal slices of 350 μm thickness containing

the hippocampal CA1 area were cut with a Vibratome Leica VT 1000 and submerged in artificial cerebrospinal fluid containing (in mM): 125 NaCl, 2.5 KCl, 1.23 NaH<sub>2</sub>PO<sub>4</sub>, 1 MgCl<sub>2</sub>, 2 CaCl<sub>2</sub>, 26 NaHCO<sub>3</sub>, 10 glucose, pH 7.4. The slices were stabilized in this solution for 1 h before electrical recording. All solutions were continuously bubbled with 95% O<sub>2</sub> and 5% CO<sub>2</sub> at room temperature.

One slice was transferred into a chamber and superfused during the experiment with artificial cerebrospinal fluid at a rate of ~2 mL/min. Whole-cell voltage-clamp recordings were performed with a PC-ONE Patch/Whole Cell Clamp (Dagan Corporation, Minneapolis, MN, United States), using a Digidata 1440A acquisition system driven with pClamp 10 (Molecular Devices, Silicon Valley, CA, United States). Patch-clamp electrodes had a resistance of 3–7 MΩ when filled with the internal solution (in mM): 140 κ-gluconate, 10 HEPES, 2 MgCl<sub>2</sub>, 0.5 CaCl<sub>2</sub>, 10 EGTA and 2 MgATP (pH 7.4). Data were stored in a PC using a Digidata 1440A AD converter, at a sampling rate of 10 kHz. Interneurons were visualized using an infrared video-microscopy system (BX51WI, Olympus Instruments, Japan) endowed with an 80x water immersion objective. Recorded interneurons were located in the *stratum radiatum* hippocampal CA1 area, and were maintained at a potential of -70 or -20 mV.

The way to explore the effects of piperidine derivatives was previously described for other substances (Vázquez-Gómez et al., 2014; López et al., 2015). Choline (Ch, 10 mM) puffs (2–5 psi, 500 ms) were applied on interneurons through a fine tip glass micropipette placed ~10 μm from the recorded cell by using a pneumatic picopump (PV830, WPI, Sarasota, FL, United States).



Thus, repeated Ch-puffs were applied at 5 min intervals before, during and after the piperidine derivative was added to the bath solution for ~10 min. In all the experiments, only one concentration of each compound was tested by cell, due to the long-lasting experiment (more than 1 h), and also just to avoid a carry-over effect. The Ch-induced current ( $I_{Ch}$ ) amplitude was measured as a function of recording time. pClamp 10 software was used to measure  $I_{Ch}$  in the absence or presence of the piperidine derivative. Origin 7 software (Microcal Software, Northampton, MA, United States) was used to analyze and graph the results. Data are presented as mean  $\pm$  standard error. Comparison of the two population means was performed by paired Student's *t*-test;  $p < 0.05$  was considered statistically significant.

## Computational Methods

Models of compounds **11a** and **12a** were built using Gaussian03 and partial charges were corrected with Electrostatic Potential methodology. Topology and parameters for the ligands was obtained with the ParamChem server, which used the CHARMM27 force field and database for organic compounds (Frisch et al., 2004; Vanommeslaeghe et al., 2010).

## Homology Modeling

To construct the extracellular domain of the rat  $\alpha 7$  nAChR, the structure of the ACh binding protein (AChBP) from *Aplysia californica* at 2.3 Å resolution was used as a template for homology modeling (code 4DBM in the Protein Data Bank) (Grimster et al., 2012).

The target protein and template were aligned with the Multalin server (Corpet, 1988). Using the software MODELLER 9v12 (Šali and Blundell, 1993), 100 runs were carried out with standard parameters and the outcomes were ranked on the basis of the internal scoring function of the software. The best model was chosen as the target model.

## Molecular Docking

To study characteristics of the principal protein–ligand interactions, molecular docking of the  $\alpha 7$  nAChRs was done using the AutoDock 4.0 software suite. In general terms, grid maps were calculated using the autogrid option and centered on the binding sites. The volumes chosen for the grid maps were made up of  $60 \times 60 \times 60$  points, with a grid-point spacing of 0.375 Å. For transmembrane domains, a grid covering the whole region was used instead. The autotors option of the software was used to define the rotating bonds in the ligand. In the Lamarckian genetic algorithm dockings, a number of individuals in a population of 1500, a maximum number of  $2.5 \times 10^6$  energy evaluations, a maximum number of 27,000 generations, a mutation rate of 0.02, and a cross-over rate of 0.80 were employed. The docked compound complexes were built using the lowest docked-energy binding positions (Morris et al., 1998).

## Molecular Dynamics Simulations

Each protein–ligand complex was solvated with water model TIP3 and submitted to molecular dynamics simulations for 20 ns

using an NPT ensemble. NAMD 2.6 software was used to perform dynamics simulations calculations. Periodic boundary conditions were applied to the system in the three coordinate directions. Pressure of one atmosphere and temperature of 310 K were maintained (Phillips et al., 2005).

## RESULTS

### Chemical Synthesis

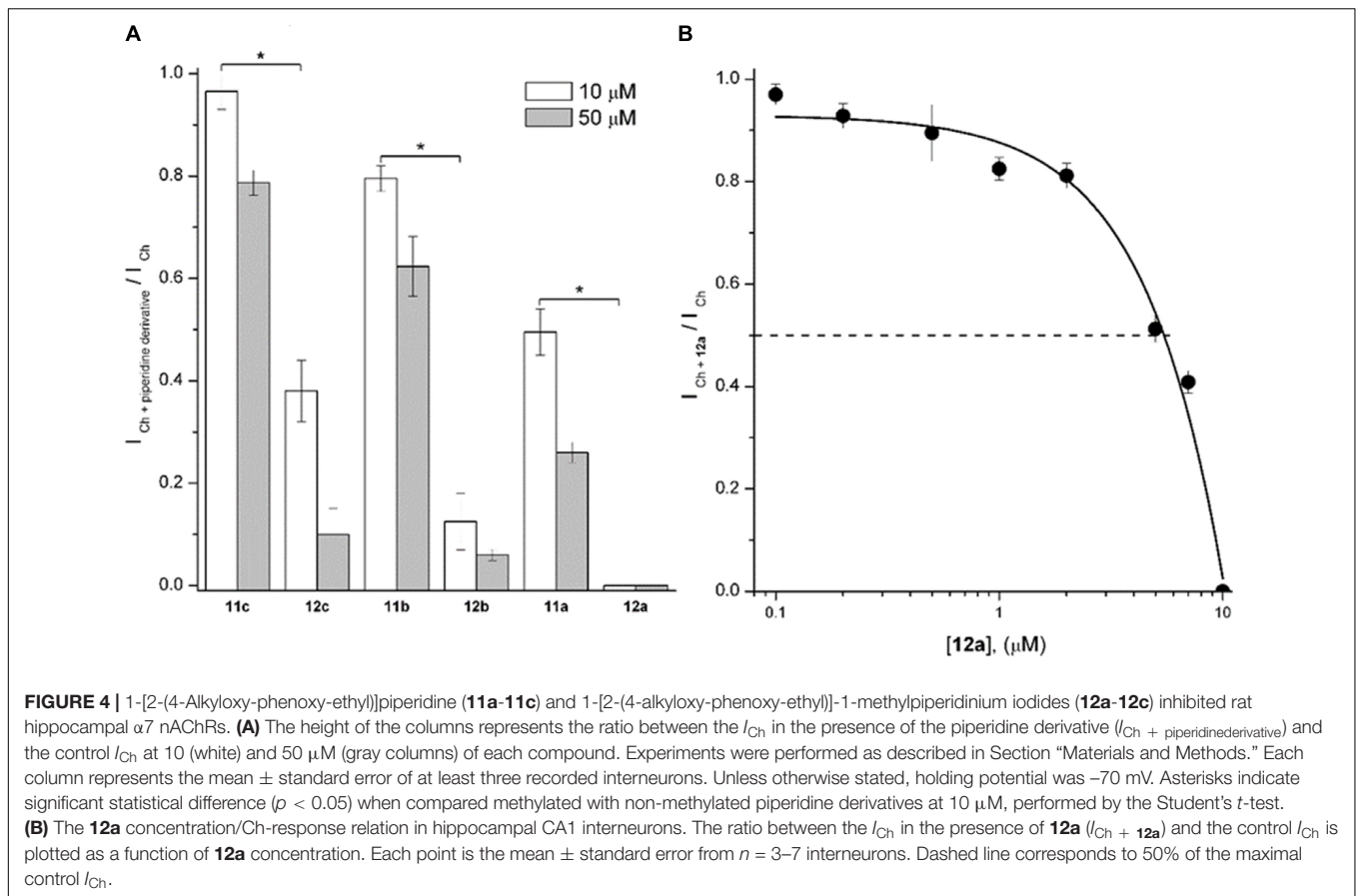
The piperidine derivatives, 1-[2-(4-alkoxy-phenoxy-ethyl)]-1-methylpiperidinium iodides, were synthesized (see **Figure 3**). A Williamson synthesis was initially used to react 4-hydroxybenzaldehyde (**Figure 3**, compound **8**) with different alkyl bromides (1-bromohexane, 1-bromoheptane, and 1-bromooctane), in a basic medium ( $K_2CO_3$ ) under reflux (Arias et al., 2013), to produce the corresponding alkoxy benzaldehydes (**9a–9c**). **9a–9c** were subsequently oxidized to their respective alkoxy phenols (**10a–10c**) by a Baeyer–Villiger reaction (Roy et al., 1999), using  $H_2O_2$  (30%),  $H_3BO_3$ , THF, and  $H_2SO_4$ , stirring for 24 h at room temperature. Afterward, the alkoxy phenols were combined with 2-piperidineethanol, using a Mitsunobu reaction (Dang et al., 2016), producing 1-[2-(4-alkoxy-phenoxy-ethyl)]piperidine derivatives **11a–11c**. These were dissolved in acetone and reacted with  $CH_3I$  for 16 h (Pérez et al., 2012), producing 1-[2-(4-alkoxy-phenoxy-ethyl)]-1-methylpiperidinium iodides **12a–12c** (quaternary ammonium salts) (Arias et al., 2013). For more details see General procedures in the Supplemental Information.

All the synthesized compounds (**Figure 3**, intermediate and final) were purified by column chromatography and their structures were confirmed by  $^1H$ -NMR and  $^{13}C$ -NMR analysis.

### Electrophysiological Recordings

Several piperidine derivatives (**Figure 3**, **11a–11c**, **12a–12c**) were tested for their effects on ion currents elicited by choline ( $I_{Ch}$ ; Alkondon et al., 1997) in interneurons from the *stratum radiatum* hippocampal CA1 area, that is, on endogenous rat  $\alpha 7$  nAChRs (Liu et al., 2012). As in previous reports, the electrical activity of native hippocampal  $\alpha 7$  nAChRs was elicited by applying local puffs of 10 mM Ch, resulting in inward ion currents decaying even in the presence of the agonist, due to receptor desensitization; and these currents were inhibited with methyllycaconitine or  $\alpha$ -bungarotoxin (Vázquez-Gómez et al., 2014; López et al., 2015).

As an initial screen, 1-[2-(4-alkoxy-phenoxy-ethyl)]piperidine (**Figure 3**, **11a–11c**) and 1-[2-(4-alkoxy-phenoxy-ethyl)]-1-methylpiperidinium iodides (**Figure 3**, **12a–12c**) were tested at 10 and 50  $\mu M$ . For each concentration, the extent of  $I_{Ch}$  inhibition depended inversely on the length of the chain, with longer chains producing less  $I_{Ch}$  inhibition. Furthermore, compounds **12a–12c** inhibited the  $I_{Ch}$  more strongly than the corresponding **11a–11c** (**Figure 4A**). Moreover, **11a** was the non-methylated compound exhibiting the highest inhibition; however, the inhibitory potency was minor than the methylated compounds. Thus, the sequence of inhibitory potency was: **12a** > **12b** > **12c** > **11a**. Compound **12a** showed the most



potent antagonistic effect on  $\alpha 7$  nAChRs: at 10  $\mu\text{M}$  this compound completely inhibited the  $I_{Ch}$  (Figure 4A). For this reason, concentrations of **12a** ranging from 0.2 to 10  $\mu\text{M}$  were tested on  $I_{Ch}$ . The inhibitory effect increased with increasing **12a** concentration (Figure 4B), attaining 50% near 5  $\mu\text{M}$  (Figure 4B).

To explore and compare the effects of **11a** and **12a**, Ch-puffs were initially applied at 5-min intervals to obtain the control  $I_{Ch}$ . In the case of **12a**, the  $I_{Ch}$  was inhibited immediately after application of 10  $\mu\text{M}$ , and the Ch response continued to be completely inhibited after washing out the **12a** (Figures 5A,C, record a2). The recovery was slow and still incomplete at  $\sim 50$  min (Figures 5A,C, record a3). In the case of **11a**, in contrast, 10  $\mu\text{M}$  moderately inhibited  $I_{Ch}$  (Figures 5B,C, record b2) and then the recovery, which was also slow and incomplete, occurred sooner (Figures 5B,C, record b3).

At a **12a** concentration near to that producing 50% inhibition (5  $\mu\text{M}$ , see Figure 4B), we explored the dependence of its effects on membrane potential, which might indicate if **12a** interacts with a site located inside the ion channel or at some other site (Woodhull, 1973; García-Colunga and Miledi, 1996). In this regard, the actions of **12a** were tested by maintaining the membrane potential of hippocampal interneurons at two different values ( $-70$  and  $-20$  mV). The inhibition the  $I_{Ch}$  was independent of membrane potential, with  $I_{Ch + 12a}/I_{Ch}$  ratios of  $0.52 \pm 0.02$  and  $0.53 \pm 0.10$  at  $-70$  and  $-20$  mV, respectively

(Figure 6), suggesting that **12a** interacts with  $\alpha 7$  nAChRs at an external domain.

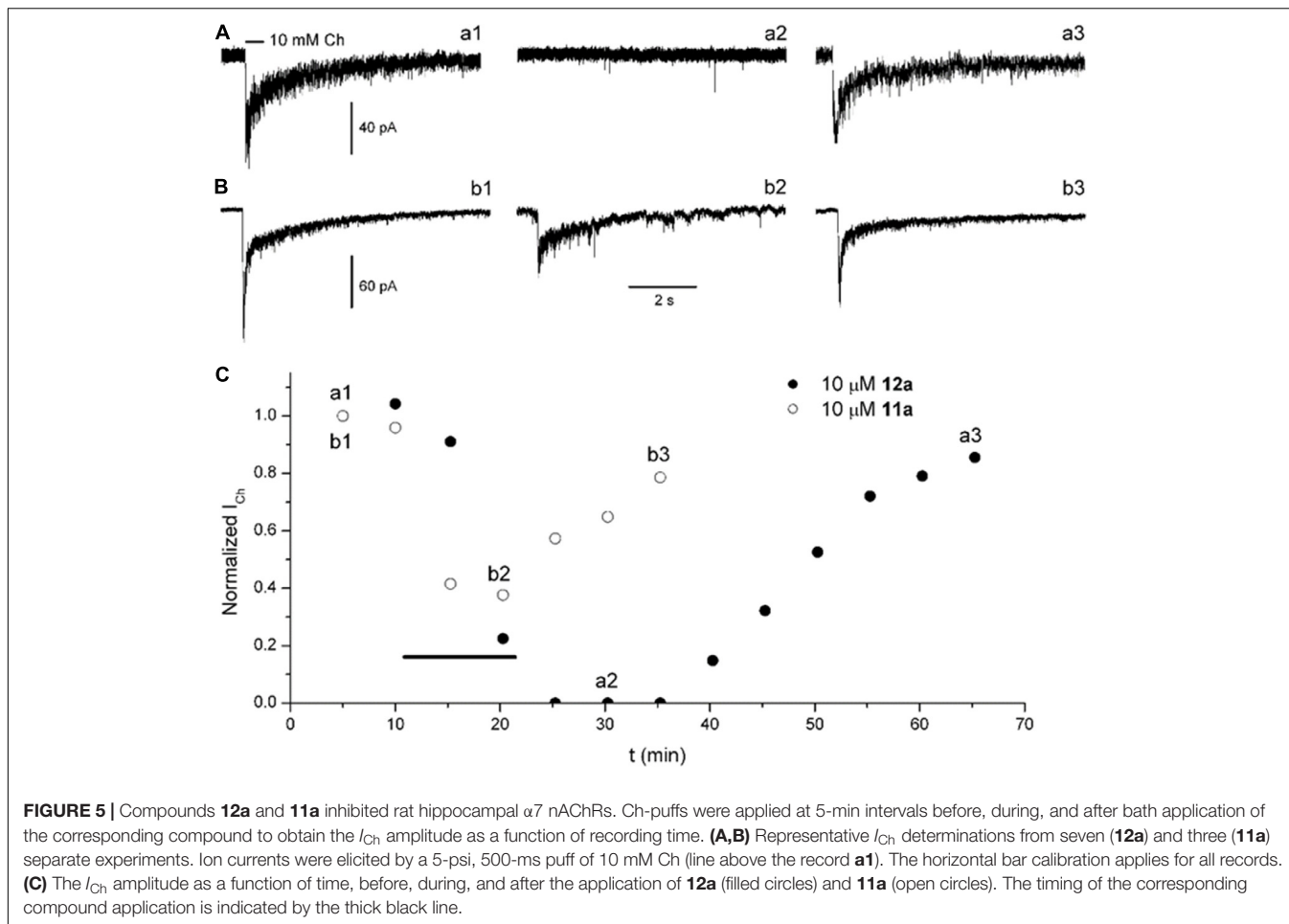
## In Silico Results

### Molecular Docking

As an aid to understanding the electrophysiological results, molecular docking studies were performed for both **11a** and **12a**. The crystal structure of the rat  $\alpha 7$  nAChR is not yet available. For this reason, a homology model was generated based on the structure of the *Aplysia californica* AChBP (Figure 7). It is important to mention that electrophysiological experiments were performed at  $\text{pH} \sim 7.4$ . Under these conditions, the piperidine nitrogen of compound **11a** is mainly protonated.

Thus, with docking studies resulted that the quaternary ammonium group of **12a** forms cation- $\pi$  interactions with the residues W147 (4.6 Å), Y91, Y187, Y191, and W58 of the principal (+)-side and the complementary (–)-side, respectively (Figure 7A). Additionally, the aliphatic chain of **12a**, located at the “para” position of the aromatic ring, presents van der Waals interactions with residues L106, Q115, Y116, and L117 of the complementary (–)-side, while the aromatic ring generates a van der Waals interaction with F103 (Figure 7A), which seems to confer selectivity for the  $\alpha 7$  nAChR (Huang et al., 2006).

On the other hand, **11a** might establish a hydrogen bond with S41 of the principal (+)-side and forms  $\pi$ - $\pi$  interactions



with W147 of the complementary (–)-side; the aliphatic chain of **11a** also forms van der Waals interactions with L106 and Q115 (Figure 7B). The calculated binding energies for derivatives **11a** and **12a** are considerably higher than that for Ch (Table 1), suggesting that these compounds interact strongly with the active site of  $\alpha 7$  nAChRs, preventing Ch from binding to the receptor, in agreement with the electrophysiological results. In this regard, the stability of their complexes might explain the slow recovery of the ability of the channel to open in response to Ch.

### Molecular Dynamics Simulations

Docking and molecular dynamic simulations are useful methodologies to obtain structural information of protein–ligand complexes. Here, the dynamics of  $\alpha 7/11a$  and  $\alpha 7/12a$  complexes were simulated during 20 ns in order to obtain information about molecular features of the systems.

#### $\alpha 7/12a$ complex

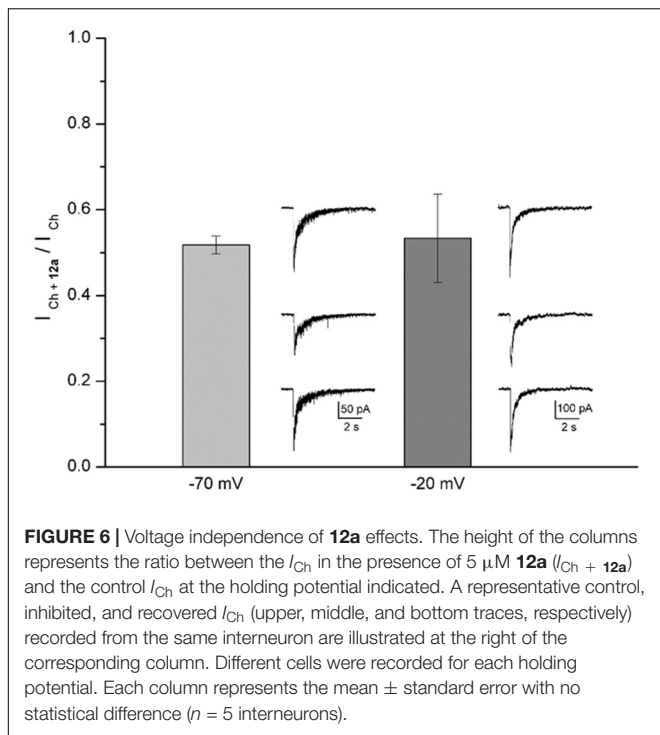
Molecular interactions from docking studies show that **12a** interacts with amino acids Y91, Y187, Y194, W147 of the principal (+)-side and W58, F103, L106, Q115, Y116, and L117 of the complementary (–) chain of the  $\alpha 7$  nAChR. In Figures 8A,B the  $\alpha 7/12a$  complex is displayed at 0 and 20 ns respectively,

interacting with amino acid residues and water molecules. During the simulation the system was stable [root-mean-square deviation (RMSD)  $\sim 3$  Å, see Supplementary Figure 14] and the aromatic cage, characteristic of nAChRs, was conserved (Figure 8C). Main interactions were selected and represented in Figure 8.

The distances from the quaternary nitrogen atom ( $N_C$ ) of **12a** to the center of the Y187, Y194, W147, Y91, and W58 were evaluated (Figure 8D). The  $N_C$ -Y187 distance (orange) shows a fluctuation associated with an interaction with a water molecule. In the case of W147 (purple) a cation– $\pi$  interaction was conserved throughout almost the total simulation time. However, between 3 and 5 ns the  $N_C$ -W147 distance increased because of a reorganization of some amino acid side chains into the cavity. After 5 ns the original distance was recovered and maintained during the remaining simulation. It is important to mention that W147 is a crucial residue for the affinity of  $\alpha 7$  nAChR ligands. Here, the distance remains at around 4.7 Å which is in accordance with Celie et al. (2004).

#### $\alpha 7/11a$ complex

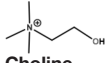
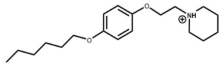
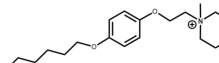
The *N*-protonated ligand **11a** was also evaluated by molecular simulation in complex with  $\alpha 7$  nAChRs. This molecule forms cation– $\pi$  interactions with W58 in the receptor cavity from



the beginning of the simulation. In addition, during the whole dynamics simulation the aliphatic chain of **11a** participates in van der Waals interactions with Q115 and L106 that help to stabilize the ligand in the cavity (**Figure 9A**).

A short hydrogen bond (1.9 Å) between the Y187 (Schjøtt et al., 1998) and the -NH of **11a** was observed at 10 ns due to the entry of a water molecule into the binding cavity. Consequently, the interaction with Y187 was broken and the cavity was solvated. Thus, W147, Y187, and Y194 from the principal (+)-chain and Q115 from the complementary (-)-chain generate a network

**TABLE 1 |** Main interactions and binding energy of the compounds Ch, **11a** and **12a** in the  $\alpha 7$  nAChR.

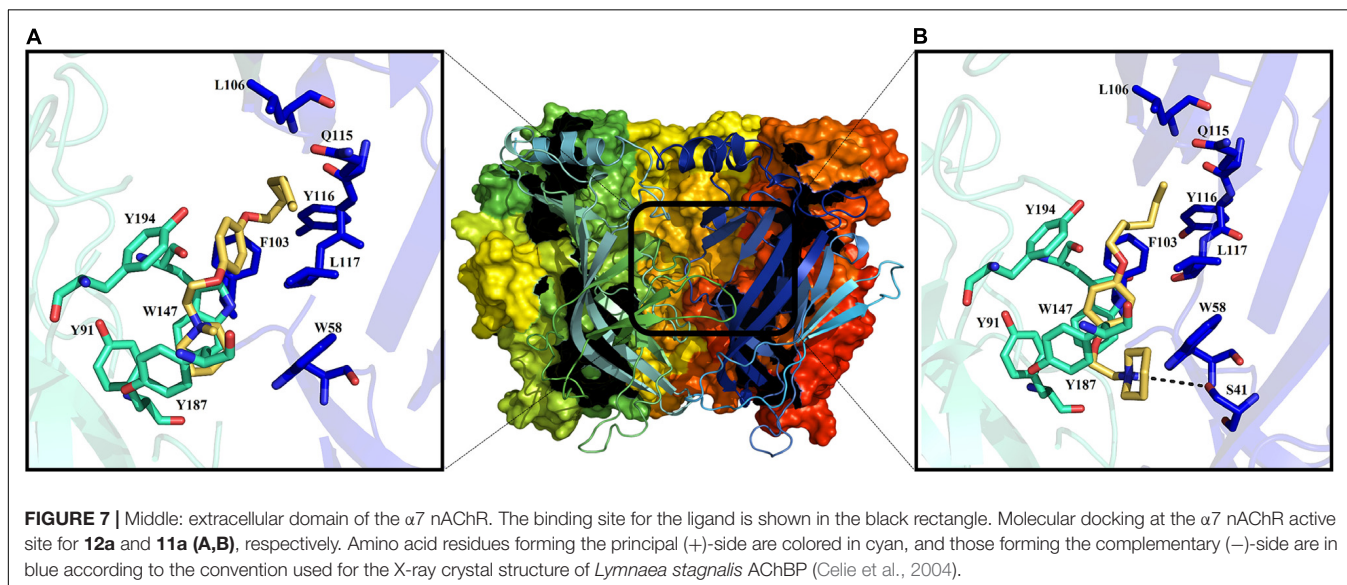
Compound	$\Delta G$ (kcal/mol)	Interaction/amino acids in the $\alpha 7$ nAChR
 Choline	-3.67	Cation- $\pi$ : (+) Y91; (+) Y187; (+) Y194; (+) W147; (-) W58 Hydrogen bond: (+) S146
 <b>11a</b>	-8.13	Cation- $\pi$ : (+) Y91; (+) Y187; (+) Y194; (+) W147; (-) W58 Hydrogen bond: (-) S41 van der Waals: (-) L106; (-) Q115
 <b>12a</b>	-8.66	Cation- $\pi$ : (+) Y91; (+) Y187; (+) Y194; (+) W147; (-) W58 van der Waals: (-) L106; (-) Q115

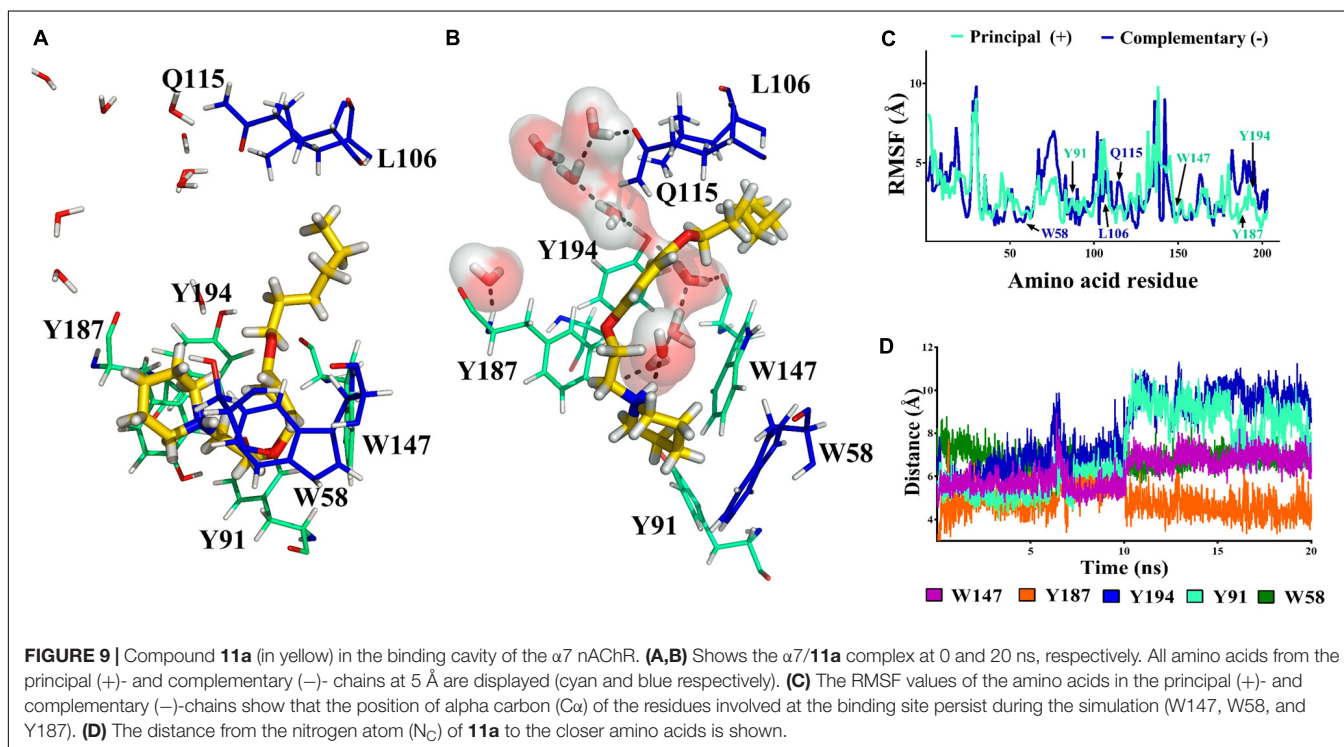
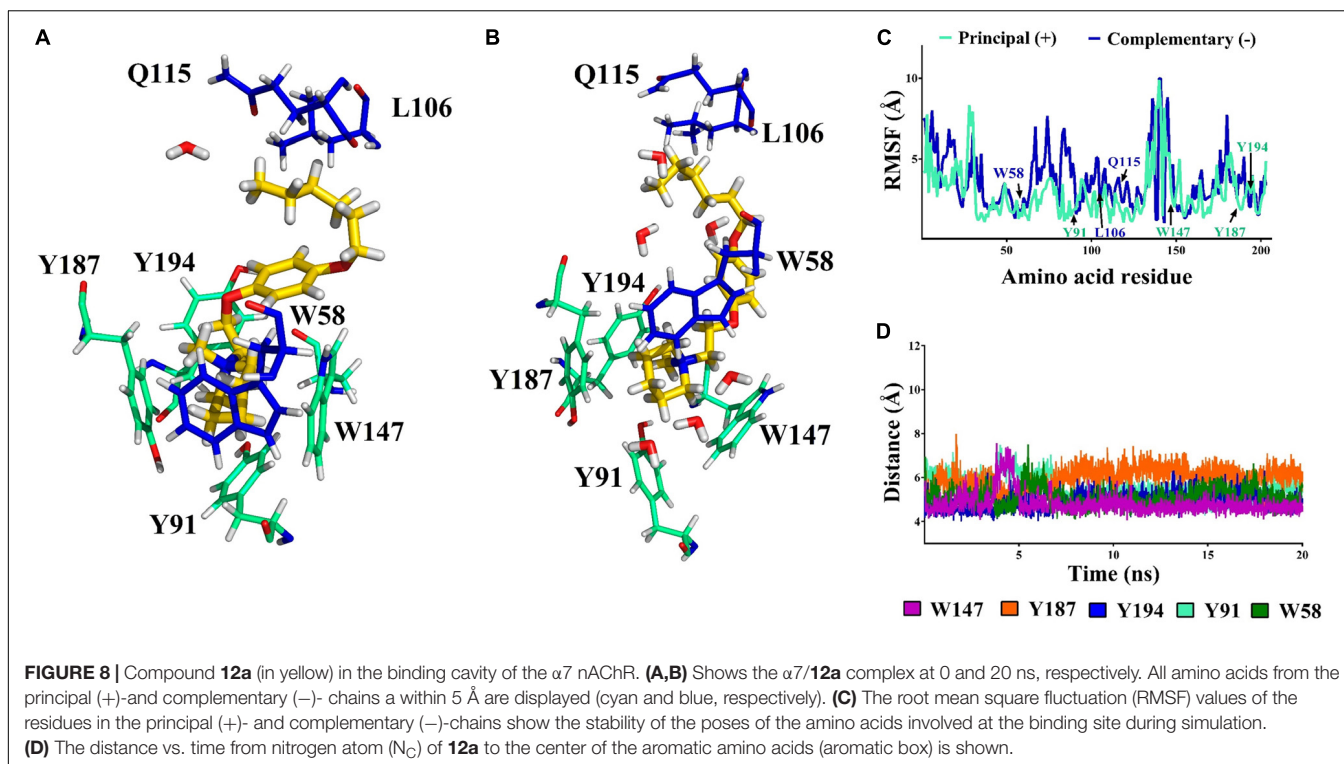
of hydrogen bonds which persists during all the simulation (**Figure 9B**). Therefore, based on the cavity solvation at 10 ns the distance between the aromatic ring of Y194, Y91 and the nitrogen of **11a** increase by more than 5 Å (**Figure 9D**) but no effect was observed on the amino acids W147, W58, and Y187 (**Figure 9C**).

#### Role of water molecules

Our atomistic simulations of **11a** and **12a** interacting with  $\alpha 7$  nAChRs show an interesting difference in the main interactions inside the cavity associated with a solvation network. In this context, a potential role of water molecules could be related to the decrease of the antagonistic effect in the derivatives studied here.

The 1-[2-(4-alkyloxy-phenoxy-ethyl)]-1-methylpiperidinium iodide derivatives (**12a-12c**) are potent antagonists of  $\alpha 7$  nAChRs, governed by a cation- $\pi$  interaction in the receptor's aromatic box. This result is consistent with the stabilization of the receptor in a non-active state. On the other hand,

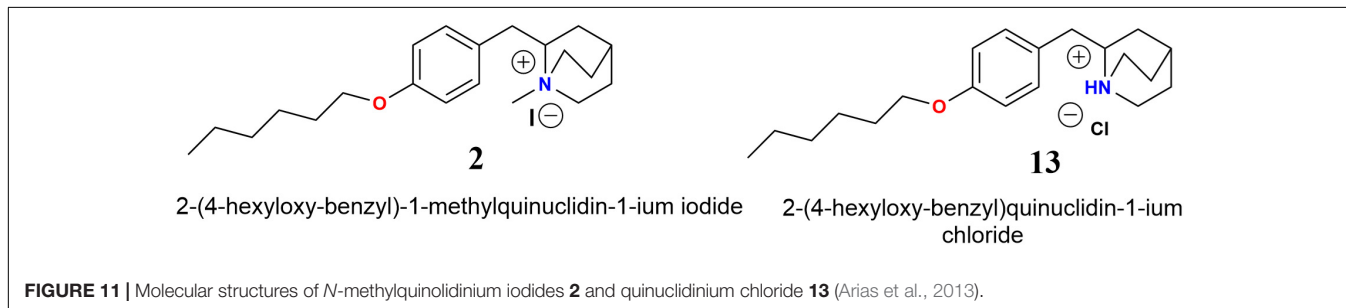
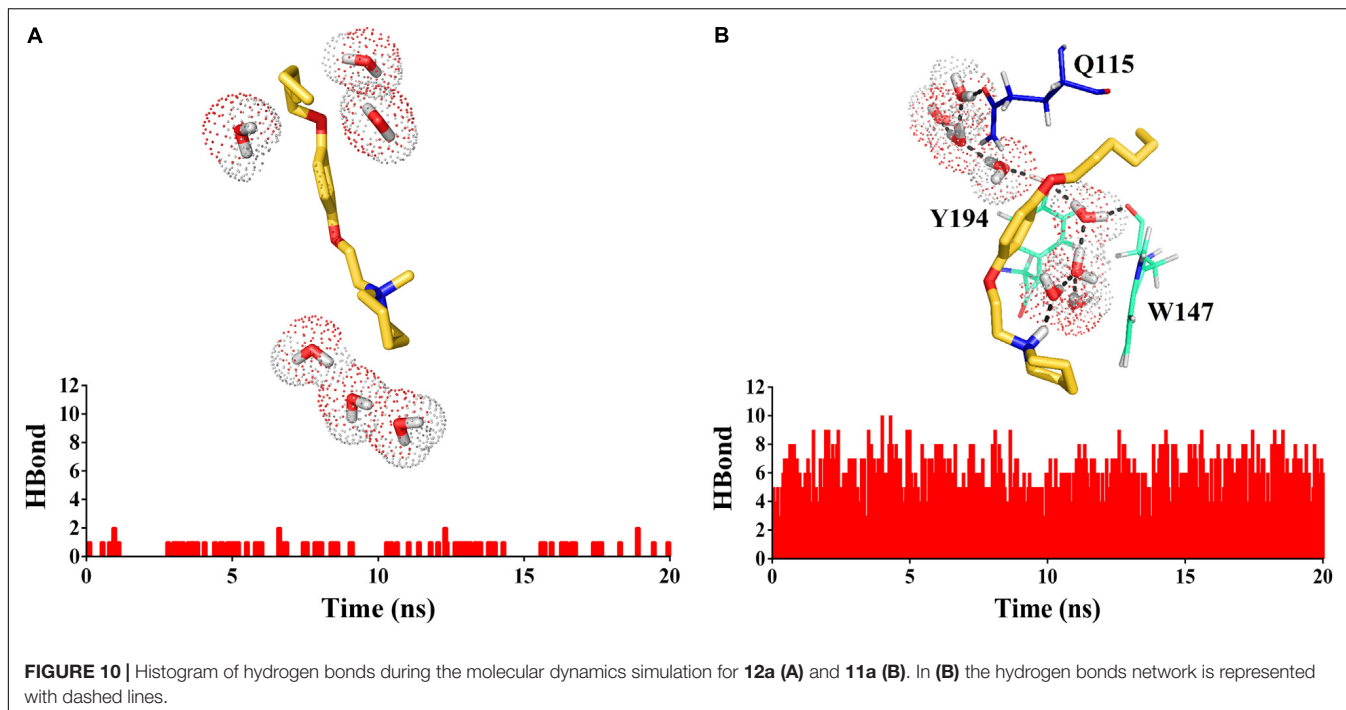




the 1-[2-(4-alkoxy-phenoxy-ethyl)]piperidine derivatives (**11a-11c**) have a hydrogen bond donator (-NH) which allows a hydrogen bond to form that interacts with Q115, W147 and Y194, generating as a consequence a more flexible cavity (**Figures 10A,B**).

## DISCUSSION

In the present work, chemical synthesis, pharmacological activity, molecular docking studies, and molecular dynamics simulations of a new series of 1-[2-(4-alkoxy-phenoxy-ethyl)]piperidines



(**11a-11c**) and 1-[2-(4-alkoxy-phenoxy-ethyl)]-1-methylpiperidinium iodides (**12a-12c**) were performed to evaluate them as possible antagonists of  $\alpha 7$  nAChRs (see **Figure 3**).

Electrophysiological recordings of the  $I_{Ch}$  in interneurons from the *stratum radiatum* hippocampal CA1 area indicated that compounds **12a-12c** inhibited the  $I_{Ch}$  more strongly than the corresponding **11a-11c**, **12a** showing the most potent antagonistic effect on  $\alpha 7$  nAChRs. Furthermore, we found that alkyl carbon chains of five atoms led to weaker  $I_{Ch}$  inhibition than compound **11a** (**Figure 4**). These results agree with previous reports, where compounds that present alkylated nitrogen incorporating an aromatic ring substituted in the “*para*” position with aliphatic chains containing six atoms of carbon are more potent antagonists for  $\alpha 7$  nAChRs than those with non-alkylated nitrogen (compounds **2** and **13**, respectively, **Figure 11**; Arias et al., 2013).

The fact that interneurons from the *stratum radiatum* hippocampal CA1 area express  $\alpha 7$ -containing nAChRs including homomeric  $\alpha 7$  and heteromeric  $\alpha 7\beta 2$  nAChRs (Wu et al., 2016), it is very likely that the  $I_{Ch}$  is the mixture of responses mediated by both subtypes of receptors. Thus, one possibility is

that **12a** inhibited both  $\alpha 7$  and  $\alpha 7\beta 2$  nAChRs. In this regard, the compound **12a** or some of its derivatives may be useful for the treatment of some diseases such as major depression and/or different types of cancer, in which  $\alpha 7$  nAChRs antagonists reverted these conditions (Egleton et al., 2008; Mineur et al., 2017).

The molecular docking studies and molecular dynamics simulations help to explain electrophysiological results. In this regard, **12a** forms cation- $\pi$  interactions with the aromatic cage of the  $\alpha 7$  nAChR, important for ligand affinity to the  $\alpha 7$  nAChR (Celie et al., 2004). In addition, the aliphatic chain of **12a** presents van der Waals interactions with F103, L106, Q115, Y116, and L117 of the complementary (–)-side. On the other hand, molecular dynamics studies showed that the *N*-methyl group of **12a** and Y194 establish a van der Waals interaction. All these interactions were conserved during almost all the molecular dynamics simulation time (20 ns), preventing both conformational changes of the receptor and its activation, which may account for the slow recovery of the  $I_{Ch}$  inhibition observed in electrophysiological assays (**Figure 8** and Supplementary Figure 15). The *N*-methyl group on the piperidinium segment

confers a positive charge in the nitrogen atom ( $N_C$ ), crucial for a cation- $\pi$  interaction with the aromatic residues into the binding cavity (high electron density aromatic box; Zhong et al., 1998). This is the same case of methylation on  $N_C$  for the nicotine pyrrolidone ring and of carbamylcholine (Celie et al., 2004).

To establish whether piperidine derivatives could interact with the heteromeric rat  $\alpha 9\alpha 10$  nAChR, a docking study was performed for the compound **12a** at the active site of this receptor [interface between  $\alpha 10(+)$  and  $\alpha 9(-)$ ; Yu et al., 2013; Azam et al., 2015]. For this purpose, we used the structure of the human  $\alpha 4\beta 2$  nAChR (Morales-Perez et al., 2016). In this regard, these studies suggest that the quaternary ammonium group of **12a** also generates cation- $\pi$  interactions with the aromatic box (Y91, Y187, Y194, W147, and W58) of the  $\alpha 9\alpha 10$  nAChR. Interestingly and in contrast with the  $\alpha 7$  nAChR (see Supplementary Figure 16A), the aliphatic chain and the aromatic ring of **12a** do not generate van der Waals interactions with the residues of the complementary (-)-side chain of the  $\alpha 9\alpha 10$  nAChR, due to the presence of D117, which generates a repulsive effect by its negative charge, causing the aliphatic chain and the aromatic ring to move away from this area. Furthermore, the aliphatic chain of **12a** presents only weak van der Waals interactions with A130 and L131 (see Supplementary Figure 16B).

These results indicate that the compound **12a** could interact at the binding site of the  $\alpha 9\alpha 10$  nAChR; however with less binding energy. This may be explained because the complementary (-)-side of the  $\alpha 9$  subunit would be very different from the complementary (-)-side of the  $\alpha 7$  subunit, which may be important for selectivity of **12a** for the  $\alpha 7$  nAChR (see Supplementary Figure 16C).

Regarding the non-methylated compound **11a**, the piperidine nitrogen of the compound is protonated at physiological pH, producing a hydrogen bond that forms a solvation network with the water molecules in the binding cavity of the  $\alpha 7$  nAChR. As in the case of **12a**, during the molecular dynamics simulations the aliphatic chain of **11a** maintains van der Waals interactions with Q115, helping to stabilize the ligand in the cavity. Thus, the difference in the interaction of **12a** and **11a** with the  $\alpha 7$  nAChR is the cation- $\pi$  interactions and hydrogen bonds, respectively, may account for the diminution of the antagonist activity, and then less  $I_{Ch}$  inhibition by **11a**. For instance, ligands with groups forming hydrogen bonds that are able to generate a solvation network with the water molecules and bind with Q115 are selective agonists of the  $\alpha 7$  nAChR (Huang et al., 2006). Consequently, one possibility is that **11a** may be, in addition to a slight antagonist, a partial agonist of the  $\alpha 7$  nAChR. However, 10  $\mu M$  **11a** applied alone both in the bath solution or with pressure puffs had no measurable effect on the membrane ion current (data not shown,  $n = 3$  for each condition), discarding an agonist action on  $\alpha 7$  nAChR.

Inhibition of the  $I_{Ch}$  by **12a**, the most potent of these antagonists of  $\alpha 7$  nAChRs, was independent of membrane potential. Moreover, the fact that complete inhibition of the  $I_{Ch}$  by **12a** occurred between 1 and 10  $\mu M$ , resulting in a sharp slope of the concentration-response relation, may indicate a high degree of cooperativity. All these suggest several binding

sites for **12a** possibly located in an external domain of the receptor, similarly as the interactions of methyllycaconitine and imipramine at chick and human  $\alpha 7$  nAChRs, respectively (Palma et al., 1996; Arias et al., 2018). These results are consistent with the present molecular docking studies and molecular dynamics simulation. Other substances interact with nAChRs in multiple sites, exhibiting complex functional modulation of the receptor; this is the case of  $Zn^{2+}$ ,  $La^{3+}$ , atropine, tacrine and the compound **2** (García-Colunga and Miledi, 1997; Zwart and Vijverberg, 1997; Moroni et al., 2008; López et al., 2015). In the case of  $(\alpha 4)_3(\beta 2)_2$  nAChRs, there are the three interacting sites for  $Zn^{2+}$  (two for inhibition and one for potentiation) (García-Colunga and Miledi, 1997; Zwart and Vijverberg, 1997; Moroni et al., 2008). Furthermore, compound **2** interacts with at least two sites in the ion channel/receptor complex: one for potentiating and another for inhibiting the  $\alpha 7$  nAChRs (López et al., 2015).

## CONCLUSION

The main purpose of this study was the designing, synthesis, and chemical characterization of a new series of 1-[2-(4-alkoxy-phenoxy-ethyl)]piperidines and 1-[2-(4-alkoxy-phenoxy-ethyl)]-1-methylpiperidinium iodides, as well as their biological and computational appraisal for evaluating them as potential ligands for the  $\alpha 7$  nAChR. With the results presented here we propose that the mode of interaction of **12a** is better than that of **11a** for having antagonist effects on the  $\alpha 7$  nAChR in a competitive fashion. *In silico* studies indicated that **12a** generated cation- $\pi$  and van der Waals interactions which were preserved throughout the simulation time. While **11a** by presenting a hydrogen bridge-forming (NH) group, generated hydrogen bonds with water molecules within the cavity, preventing the formation of a cation- $\pi$  interaction. Water molecules inside the receptor cavity would play an important role in decreasing antagonistic activity in non-methylated derivatives, due to the formation of hydrogen bonds, which would lead to a more flexible cavity. We hope that this study may lead to development of new compounds with antagonistic properties at  $\alpha 7$  nAChRs that might be clinically useful for the treatment of pathologies associated with these receptors, including neuropsychiatric disorders and different types of cancer.

## AUTHOR CONTRIBUTIONS

JJL and JG-C: performed the research and analyzed the data. JG-C, EP, and AF supervised the investigation. All the authors designed the research, wrote, and critically revised the manuscript.

## FUNDING

We are grateful for financial support from the Fondo Nacional para el Desarrollo Científico y Tecnológico, Chile (FONDECYT, postdoctorado 2017 No. 3170061) to JJL, and the FONDECYT

regular 1161375 to AF; the Dirección General de Asuntos del Personal Académico, UNAM for a DGAPA grant IN205016 and a PASPA grant to JG-C.

## ACKNOWLEDGMENTS

We are very grateful to professor Bruce K. Cassels for reviewing the manuscript. We thank Dr. Elizabeth Vázquez-Gómez for

technical assistance, and Martín García-Servín for his assistance in taking care of the rats.

## SUPPLEMENTARY MATERIAL

The Supplementary Material for this article can be found online at: <https://www.frontiersin.org/articles/10.3389/fphar.2018.00744/full#supplementary-material>

## REFERENCES

- Albuquerque, E. X., Pereira, E. F. R., Alkondon, M., and Rogers, S. W. (2009). Mammalian nicotinic acetylcholine receptors: from structure to function. *Physiol. Rev.* 89, 73–120. doi: 10.1152/physrev.00015.2008
- Alkondon, M., Pereira, E., Cortes, W., Maelicke, A., and Albuquerque, E. (1997). Choline is a selective agonist of  $\alpha 7$  nicotinic acetylcholine receptors in the rat brain neurons. *Eur. J. Neurosci.* 9, 2734–2742. doi: 10.1111/j.1460-9568.1997.tb01702.x
- Arias, H. R., López, J. J., Feuerbach, D., Fierro, A., Ortells, M. O., and Pérez, E. G. (2013). Novel 2-(substituted benzyl)quinuclidines inhibit human  $\alpha 7$  and  $\alpha 4\beta 2$  nicotinic receptors by different mechanisms. *Int. J. Biochem. Cell Biol.* 45, 2420–2430. doi: 10.1016/j.biocel.2013.08.003
- Arias, H. R., Vázquez-Gómez, E., Hernández-Abrego, A., Gallino, S., Feuerbach, D., Ortells, M. O., et al. (2018). Tricyclic antidepressants inhibit hippocampal  $\alpha 7^*$  and  $\alpha 9\alpha 10$  nicotinic acetylcholine receptors by different mechanisms. *Int. J. Biochem. Cell Biol.* 25, 1–10. doi: 10.1016/j.biocel.2018.04.017
- Azam, L., Papakyriakou, A., Zouridakis, M., Giastas, P., Tzartos, S. J., and McIntosh, J. M. (2015). Molecular interaction of  $\alpha$ -conotoxin RgIA with the rat  $\alpha 9\alpha 10$  nicotinic acetylcholine receptor. *Mol. Pharmacol.* 87, 855–864. doi: 10.1124/mol.114.096511
- Blum, A. P., Lester, H. A., and Dougherty, D. A. (2010). Nicotinic pharmacophore: the pyridine N of nicotine and carbonyl of acetylcholine hydrogen bond across a subunit interface to a backbone NH. *Proc. Natl. Acad. Sci. U.S.A.* 107, 13206–13211. doi: 10.1073/pnas.1007140107
- Celie, P. H. N., van Rossum-Fikkert, S. E., van Dijk, W. J., Brejc, K., Smit, A. B., and Sixma, T. K. (2004). Nicotine and carbamylcholine binding to nicotinic acetylcholine receptors as studied in AChBP crystal structures. *Neuron* 41, 907–914. doi: 10.1016/S0896-6273(04)00115-1
- Cooke, J. P., and Bitterman, H. (2004). Nicotine and angiogenesis: a new paradigm for tobacco-related diseases. *Ann. Med.* 36, 33–40. doi: 10.1080/07853890310017576
- Corpet, F. (1988). Multiple sequence alignment with hierarchical clustering. *Nucleic Acids Res.* 16, 10881–10890. doi: 10.1093/nar/16.22.10881
- Crooks, P. A., Ravard, A., Wilkins, L. H., Teng, L. H., Buxton, S. T., and Dwoskin, L. P. (1995). Inhibition of nicotine-evoked [3H]dopamine release by pyridino N-substituted nicotine analogs: a new class of nicotinic antagonist. *Drug Dev. Res.* 36, 91–102. doi: 10.1002/ddr.430360204
- Dang, N., Meng, X., and Song, H. (2016). Nicotinic acetylcholine receptors and cancer. *Biomed. Rep.* 4, 515–518. doi: 10.3892/br.2016.625
- Dasgupta, P., Rastogi, S., Pillai, S., Ordóñez-Ercan, D., Morris, M., Haura, E., et al. (2006). Nicotine induces cell proliferation by  $\beta$ -arrestin-mediated activation of Src and Rb-Raf-1 pathways. *J. Clin. Invest.* 116, 2208–2217. doi: 10.1172/JCI28164
- Dineley, K. T., Pandya, A. A., and Yakel, J. L. (2015). Nicotinic ACh receptors as therapeutic targets in CNS disorders. *Trends Pharmacol. Sci.* 36, 96–108. doi: 10.1016/j.tips.2014.12.002
- Dunbar, G. C., Kuchibhatla, R. V., and Lee, G. (2011). A randomized double-blind study comparing 25 and 50 mg TC-1734 (AZD3480) with placebo, in older subjects with age-associated memory impairment. *J. Psychopharmacol.* 25, 1020–1029. doi: 10.1177/0269881110367727
- Dwoskin, L. P., and Crooks, P. A. (2001). Competitive neuronal nicotinic receptor antagonists: a new direction for drug discovery. *J. Pharmacol. Exp. Ther.* 298, 395–402. doi: 10.1016/j.bcp.2013.07.021
- Egleton, R. D., Brown, K. C., and Dasgupta, P. (2008). Nicotinic acetylcholine receptors in cancer: multiple roles in proliferation and inhibition of apoptosis. *Trends Pharmacol. Sci.* 29, 151–158. doi: 10.1016/j.tips.2007.12.006
- Frisch, M. J., Trucks, G. W., Schlegel, H. B., Scuseria, G. E., Robb, M. A., Cheeseman, J. R., et al. (2004). Gaussian 03, revision C.02. *J. Comput. Chem.* 24, 1748–1757.
- Gahring, L. C., Myers, E. J., Dunn, D. M., Weiss, R. B., and Rogers, S. W. (2017). Nicotinic alpha 7 receptor expression and modulation of the lung epithelial response to lipopolysaccharide. *PLoS One* 12:e0175367. doi: 10.1371/journal.pone.0175367
- García-Colunga, J., and Miledi, R. (1996). Serotonergic modulation of muscle acetylcholine receptors of different subunit composition. *Proc. Natl. Acad. Sci. U.S.A.* 93, 3990–3994. doi: 10.1073/pnas.93.9.3990
- García-Colunga, J., and Miledi, R. (1997). Opposite effects of lanthanum on different types of nicotinic acetylcholine receptors. *Neuroreport* 8, 3293–3296. doi: 10.1097/00001756-199710200-00020
- Ghiron, C., Haydar, S. N., Aschmies, S., Bothmann, H., Castaldo, C., Cocconcelli, G., et al. (2010). Novel  $\alpha 7$  nicotinic acetylcholine receptor agonists containing a urea moiety: identification and characterization of the potent, selective, and orally efficacious agonist 1-[6-(4-fluorophenyl)pyridin-3-yl]-3-(4-piperidin-1-ylbutyl) urea (SEN34625/WYE-103914). *J. Med. Chem.* 53, 4379–4389. doi: 10.1021/jm901692q
- Gotti, C., Clementi, F., Fornari, A., Gaimarri, A., Guiducci, S., Manfredi, I., et al. (2009). Structural and functional diversity of native brain neuronal nicotinic receptors. *Biochem. Pharmacol.* 78, 703–711. doi: 10.1016/j.bcp.2009.05.024
- Grimster, N. P., Stump, B., Fotsing, J. R., Weide, T., Talley, T. T., and Yamauchi, J. G. (2012). Generation of candidate ligands for nicotinic acetylcholine receptors via in situ click chemistry with a soluble acetylcholine binding protein template. *J. Am. Chem. Soc.* 134, 6732–6740. doi: 10.1021/ja3001858
- Heeschen, C., Weis, M., Aicher, A., Dimmeler, S., and Cooke, J. P. (2002). A novel angiogenic pathway mediated by nonneuronal nicotinic acetylcholine receptors. *J. Clin. Invest.* 110, 527–536. doi: 10.1172/JCI200214676
- Huang, X., Zheng, F., Chen, X., Crooks, P. A., Dwoskin, L. P., and Zhan, C. G. (2006). Modeling subtype-selective agonists binding with  $\alpha 4\beta 2$  and  $\alpha 7$  nicotinic acetylcholine receptors: effects of local binding and long-range electrostatic interactions. *J. Med. Chem.* 49, 7661–7674. doi: 10.1021/jm0606701
- Innocent, N., Livingstone, P. D., Hone, A., Kimura, A., Young, T., Whiteaker, P., et al. (2008).  $\alpha$ Conotoxin Arenatus IB[V11L,V16D] Is a potent and selective antagonist at rat and human native  $\alpha 7$  nicotinic acetylcholine receptors. *J. Pharmacol. Exp. Ther.* 327, 529–537. doi: 10.1124/jpet.108.142943
- Lester, H. A., Dibas, M. I., Dahan, D. S., Leite, J. F., and Dougherty, D. A. (2004). Cys-loop receptors: new twists and turns. *Trends Neurosci.* 27, 329–336. doi: 10.1016/j.tins.2004.04.002
- Liu, Q., Huang, Y., Shen, J., Steffensen, S., and Wu, J. (2012). Functional  $\alpha 7\beta 2$  nicotinic acetylcholine receptors expressed in hippocampal interneurons exhibit high sensitivity to pathological level of amyloid  $\beta$  peptides. *BMC Neurosci.* 13:155. doi: 10.1186/1471-2202-13-155
- López, J. J., Pérez, E. G., and García-Colunga, J. (2015). Dual effects of a 2-benzylquinuclidinium derivative on  $\alpha 7$ -containing nicotinic acetylcholine receptors in rat hippocampal interneurons. *Neurosci. Lett.* 607, 35–39. doi: 10.1016/j.neulet.2015.09.016
- Mazurov, A. A., Speake, J. D., and Yohannes, D. (2011). Discovery and development of  $\alpha 7$  nicotinic acetylcholine receptor modulators. *J. Med. Chem.* 54, 7943–7961. doi: 10.1021/jm2007672
- Mineur, Y. S., Mose, T. N., Blakeman, S., and Picciotto, M. R. (2017). Hippocampal  $\alpha 7$  nicotinic ACh receptors contribute to modulation of depression-like

- behaviour in C57BL/6J mice. *Br. J. Pharmacol.* 175, 1903–1914. doi: 10.1111/bph.13769
- Morales-Perez, C. L., Noviello, C. M., and Hibbs, R. E. (2016). X-ray structure of the human  $\alpha 4\beta 2$  nicotinic receptor. *Nature* 538, 411–415. doi: 10.1038/nature19785
- Moroni, M., Vijayan, R., Carbone, A., Zwart, R., Biggin, P. C., and Bermudez, I. (2008). Non-agonist-binding subunit interfaces confer distinct functional signatures to the alternate stoichiometries of the  $\alpha 4\beta 2$  nicotinic receptor: an  $\alpha 4$ - $\alpha 4$  interface is required for Zn<sup>2+</sup> + potentiation. *J. Neurosci.* 28, 6884–6894. doi: 10.1523/JNEUROSCI.1228-08.2008
- Morris, G. M., Goodsell, D. S., Halliday, R. S., Huey, R., Hart, W. E., Belew, R. K., et al. (1998). Automated docking using a Lamarckian genetic algorithm and empirical binding free energy function. *J. Comput. Chem.* 19, 1639–1662. doi: 10.1002/(SICI)1096-987X(19981115)19:14<1639::AID-JCC10>3.0.CO;2-B
- Olsen, J. A., Balle, T., Gajhede, M., Ahring, P. K., and Kastrop, J. S. (2014). Molecular recognition of neurotransmitter acetylcholine by an acetylcholine binding protein reveals determinants of binding to nicotinic acetylcholine receptors. *PLoS One* 9:e91232. doi: 10.1371/journal.pone.0091232
- Palma, E., Bertrand, S., Binzoni, T., and Bertrand, D. (1996). Neuronal nicotinic  $\alpha 7$  receptor expressed in *Xenopus* oocytes presents five putative binding sites for methyllycaconitine. *J. Physiol.* 491, 151–161. doi: 10.1113/jphysiol.1996.sp021203
- Peng, Y., Zhang, Q., Snyder, G. L., Zhu, H., Yao, W., Tomesch, J., et al. (2010). Discovery of novel  $\alpha 7$  nicotinic receptor antagonists. *Bioorg. Med. Chem. Lett.* 20, 4825–4830. doi: 10.1016/j.bmcl.2010.06.103
- Pérez, E. G., Cassels, B. K., Eibl, C., and Gündisch, D. (2012). Synthesis and evaluation of N1-alkylindole-3-ylalkylammonium compounds as nicotinic acetylcholine receptor ligands. *Bioorg. Med. Chem. Lett.* 20, 3719–3727. doi: 10.1016/j.bmcl.2012.04.050
- Pérez, E. G., Ocampo, C., Feuerbach, D., López, J. J., Morelo, G. L., Tapia, R. A., et al. (2013). Novel 1-(1-benzyl-1H-indol-3-yl)-N,N,N-trimethylmethanaminium iodides are competitive antagonists for the human  $\alpha 4\beta 2$  and  $\alpha 7$  nicotinic acetylcholine receptors. *Med. Chem. Commun.* 4, 1166–1170. doi: 10.1039/c3md00042g
- Peters, D., Eriksen, B. L., Nielsen, E. O., Scheel-Krüger, J., and Olsen, G. M. (2006). inventor; Neurosearch A/S, assignee. Novel 8-aza-bicyclo[3.2.1]octane derivatives and their use as monoamine neurotransmitter re-uptake inhibitors. United States Patent WO2004072075 A1.
- Phillips, J. C., Braun, R., Wang, W., Gumbart, J., Tajkhorshid, E., and Villa, E. (2005). Scalable molecular dynamics with NAMD. *J. Comput. Chem.* 26, 1781–1802. doi: 10.1002/jcc.20289
- Romanelli, M. N., Gratteri, P., Guandalini, L., Martini, E., Bonaccini, C., and Gualtieri, F. (2007). Central nicotinic receptors: structure, function, ligands, and therapeutic potential. *Chem. Med. Chem.* 2, 746–767. doi: 10.1002/cmcd.200600207
- Roy, A., Reddy, K. R., Mohanta, P. K., Ila, H., and Junjappat, H. (1999). Hydrogen peroxide/boric acid: an efficient system for oxidation of aromatic aldehydes and ketones to phenols. *Synth. Commun.* 29, 3781–3791. doi: 10.1080/00397919908086017
- Šali, A., and Blundell, T. L. (1993). Comparative protein modelling by satisfaction of spatial restraints. *J. Mol. Biol.* 234, 779–815. doi: 10.1006/jmbi.1993.1626
- Schiott, B., Iversen, B. B., Madsen, G. K., Larsen, F. K., and Bruice, T. C. (1998). On the electronic nature of low-barrier hydrogen bonds in enzymatic reactions. *Proc. Natl. Acad. Sci. U.S.A.* 95, 12799–12802. doi: 10.1073/pnas.95.22.12799
- Terry, A. V. Jr., Callahan, P. M., and Hernandez, C. M. (2015). Nicotinic ligands as multifunctional agents for the treatment of neuropsychiatric disorders. *Biochem. Pharmacol.* 97, 388–398. doi: 10.1016/j.bcp.2015.07.027
- Trombino, S., Cesario, A., Margaritora, S., Granone, P., Motta, G., Falugi, C., et al. (2004).  $\alpha 7$ -Nicotinic acetylcholine receptors affect growth regulation of human mesothelioma cells: role of mitogen activated protein kinase pathway. *Cancer Res.* 64, 135–145. doi: 10.1158/0008-5472.CAN-03-1672
- Vanommleslaeghe, K., Hatcher, E., Acharya, C., Kundu, S., Zhong, S., and Shim, J. (2010). CHARMM General force field: a force field for drug-like molecules compatible with the CHARMM all-atom additive biological force field. *J. Comput. Chem.* 31, 671–690. doi: 10.1002/jcc.21367
- Vázquez-Gómez, E., Arias, H. R., Feuerbach, D., Miranda-Morales, M., Mihăilescu, S., Targowska-Duda, K. M., et al. (2014). Bupropion-induced inhibition of  $\alpha 7$  nicotinic acetylcholine receptors expressed in heterologous cells and neurons from dorsal raphe nucleus and hippocampus. *Eur. J. Pharmacol.* 740, 103–111. doi: 10.1016/j.ejphar.2014.06.059
- Wilkins, L. H., Grinevich, V. P., Ayers, J. T., Crooks, P. A., and Dvoskin, L. P. (2002). N-n-alkylnicotinium analogs, a novel class of nicotinic receptor antagonists: interaction with  $\alpha 4\beta 2^*$  and  $\alpha 7^*$  neuronal nicotinic receptors. *J. Pharmacol. Exp. Ther.* 304, 400–410. doi: 10.1124/jpet.102.043349
- Wong, H. P., Yu, L., Lam, E. K. Y., Tai, E. K. K., Wu, W. K. K., and Cho, C. H. (2007). Nicotine promotes cell proliferation via  $\alpha 7$ -nicotinic acetylcholine receptor and catecholamine-synthesizing enzymes-mediated pathway in human colon adenocarcinoma HT-29 cells. *Toxicol. Appl. Pharmacol.* 221, 261–267. doi: 10.1016/j.taap.2007.04.002
- Woodhull, A. M. (1973). Ionic blockage of sodium channels in nerve. *J. Gen. Physiol.* 61, 687–708. doi: 10.1085/jgp.61.6.687
- Wu, J., Liu, Q., Tang, P., Mikkelsen, J. D., Shen, J., Whiteaker, P., et al. (2016). Heteromeric  $\alpha 7\beta 2$  nicotinic acetylcholine receptors in the brain. *Trends Pharmacol. Sci.* 37, 562–574. doi: 10.1016/j.tips.2016.03.005
- Yu, R., Kompella, S. N., Adams, D. J., Craik, D. J., and Kaas, Q. (2013). Determination of the  $\alpha$ -conotoxin Vc1.1 binding site on the  $\alpha 9\alpha 10$  nicotinic acetylcholine receptor. *J. Med. Chem.* 56, 3557–3567. doi: 10.1021/jm400041h
- Zhong, W., Gallivan, J. P., Zhang, Y., Li, L., Lester, H. A., and Dougherty, D. A. (1998). From ab initio quantum mechanics to molecular neurobiology: a cation- $\pi$  binding site in the nicotinic receptor. *Proc. Natl. Acad. Sci. U.S.A.* 95, 12088–12093. doi: 10.1073/pnas.95.21.12088
- Zoli, M., Pucci, S., Vilella, A., and Gotti, C. (2017). Neuronal and extraneuronal nicotinic acetylcholine receptors. *Curr. Neuropharmacol.* 15, 1–11. doi: 10.2174/1570159X15666170912110450
- Zwart, R., and Vijverberg, H. P. (1997). Potentiation and inhibition of neuronal nicotinic receptors by atropine: competitive and noncompetitive effects. *Mol. Pharmacol.* 52, 886–895. doi: 10.1124/mol.52.5.886

**Conflict of Interest Statement:** The authors declare that the research was conducted in the absence of any commercial or financial relationships that could be construed as a potential conflict of interest.

Copyright © 2018 López, García-Colunga, Pérez and Fierro. This is an open-access article distributed under the terms of the Creative Commons Attribution License (CC BY). The use, distribution or reproduction in other forums is permitted, provided the original author(s) and the copyright owner(s) are credited and that the original publication in this journal is cited, in accordance with accepted academic practice. No use, distribution or reproduction is permitted which does not comply with these terms.